Applied Physics Letters

Spatially resolved tunneling spectroscopy of superconducting wires with artificial pinning centers

Cite as: Appl. Phys. Lett. **72**, 480 (1998); https://doi.org/10.1063/1.120792
Submitted: 20 June 1997 . Accepted: 20 November 1997 . Published Online: 04 June 1998

Y. Levi, O. Millo, N. D. Rizzo, D. E. Prober, and L. R. Motowidlo

Spatially resolved tunneling spectroscopy of superconducting wires with artificial pinning centers

Y. Levi and O. Millo[a)]
Racah Institute of Physics, The Hebrew University, Jerusalem 91904, Israel

N. D. Rizzo[b)] and D. E. Prober
Applied Physics, Yale University, New Haven, Connecticut 06520-8284

L. R. Motowidlo
IGC-AS, Waterbury, Connecticut 06704

(Received 20 June 1997; accepted for publication 20 November 1997)

We used scanning tunneling microscopy and spectroscopy to study with nanometer resolution the spatial variation of superconductivity in the vicinity of the interface between normal and superconductor regions. The samples were novel superconducting wires consisting of ordered arrays of sub-micron diameter normal metal filaments, either Cu or Ni, embedded in a NbTi superconducting matrix. By taking topographic images simultaneously with current–voltage curves, we obtain information about the local quasi-particle density of states on both sides of the interface.
 [S0003-6951(98)00604-4]

''Artificial pinning centers (APCs) wires'' are superconducting wires specially engineered to enhance magnetic flux pinning in order to increase the critical current at high magnetic fields. While in the conventional technique flux-pins are introduced by creating random defects along the wire, the APC approach introduces chosen pin materials (normal or magnetic) in a well defined ordered filamentary configuration. These wires have already demonstrated higher critical currents than those produced with conventional processing.[1,2] Understanding their microscopic properties may help to further optimize their performance. In particular, it is instructive to study the variation of superconductivity in the vicinity of normal metal (N)–superconductor (S) boundaries. The advent of scanning tunneling microscopy (STM) now enables such local studies of electronic properties.

Two factors may affect the local S properties near the N-S interface: material intermixing and the proximity effect (PE), namely the mutual effect of N in good electrical contact with S. The PE has been studied for over 3 decades[3,4] but has recently met a revival due to technological advancements which afford experiments revealing novel mesoscopic effects.[5–7] One is especially intrigued by the microscopic variations of the condensate and the pair potential in vicinity of the N-S boundary, and the way they are reflected in the quasi-particle density of states (DOS). The vast majority of the experiments designed to probe the PE rely on *macroscopic* measurements (resistivity, magnetization, etc.), and thus lose important information on the local behavior. Tunneling spectroscopy has also been extensively employed, using relatively *large-area* tunnel junctions fabricated *perpendicular* to the N-S interface.[4]

In the past few years some high spatial resolution tunneling spectroscopy measurements of the PE have already been performed.[8–10] However, in these studies tunneling occurred through very thin N islands deposited on top of a bulk superconductor,[8] or in granular samples having poor electrical contact between adjacent grains.[10] To the best of our knowledge, spatially resolved measurements where the tunneling current is *parallel* to the interfaces between ''semi-infinite'' slabs of materials in good electrical contact (see inset of Fig. 1) have not previously been conducted. This letter presents the results of such studies, and demonstrates their utility in accessing microscopic information in material science.

The specimens used in our study are APC wires manufactured at IGC-Advanced Superconductors, whose method of manufacture and electrical properties at various magnetic fields are reported elsewhere.[1] A key issue here, with respect to studies of the PE, is that there is good electrical contact between the different constituents of the wire.[5] Moreover, the sub-micron diameter of each individual filament, along with its ''infinite'' length, make it an ideal system for our STM measurements (performed along the cross section of the wire). On the other hand, one must take into account that during the fabrication process *some* material intermixing occurs at the interfaces (although care was taken to design the wires with immiscible materials). This intermixing may result in a significant ''blurring'' of the interfaces.

We used two types of wires. The first [Figs. 1 and 3(a)]

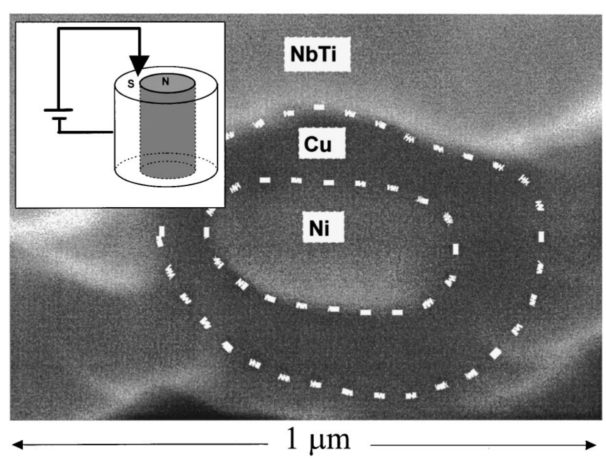

FIG. 1. A SEM micrograph focusing on an individual Ni island-pin consisting of a Ni core (center), a Cu sleeve (dark ring), and NbTi superconductor (bright surface all around). (Inset) Schematic of the experimental setup. The black arrow represents the STM tip, and tunneling is parallel to the interface between the wire constituents.

[a)]Electronic mail: milode@vms.huji.ac.il
[b)]Present address: NIST 814.05, Boulder, CO 80303.

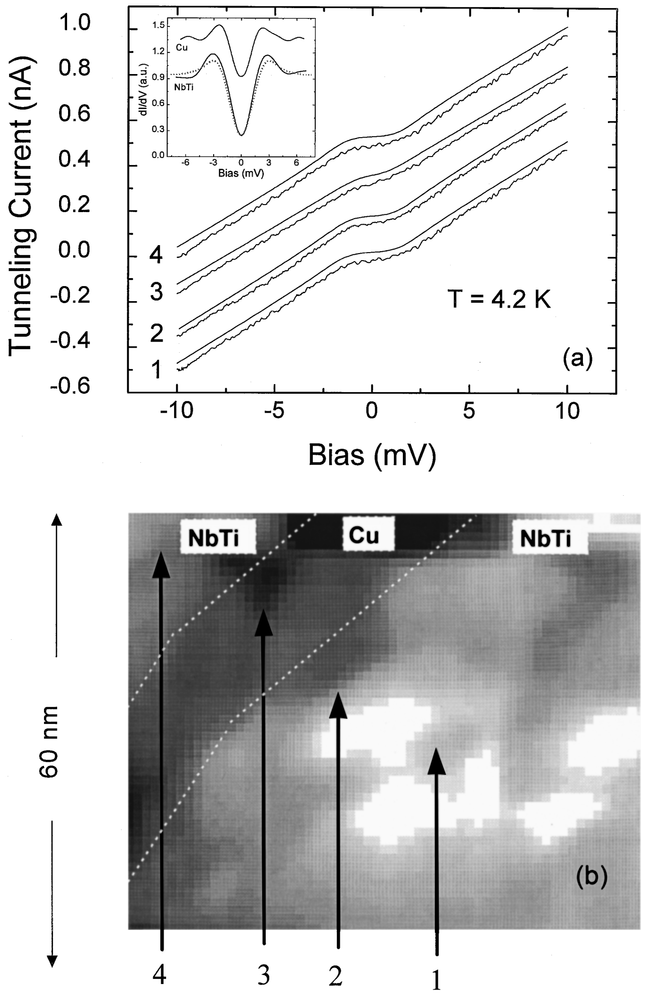

FIG. 2. (a) Four $I-V$ characteristics taken at different lateral tip positions along a Cu barrier-pin wire. The smooth lines were calculated using Dynes' formula. For curves 1–4, $\Delta = 1.55$, 1.45, 0.8, and 1.3 meV, respectively. Curves are vertically displaced for clarity. (b) Detail of a STM topographic image of the wire's cross section, showing the locations where the curves in (a) were taken. Curves 1, 2, and 4 are taken on two NbTi regions that are separated by a Cu pin, where curve 3 was taken. The boundaries between different materials are designated by dashed lines. (Inset) Normalized dI/dV traces taken on Cu (top) and deep on NbTi (bottom, solid line). The dotted line is a theoretical fit, with $\Delta = 1.55$ meV.

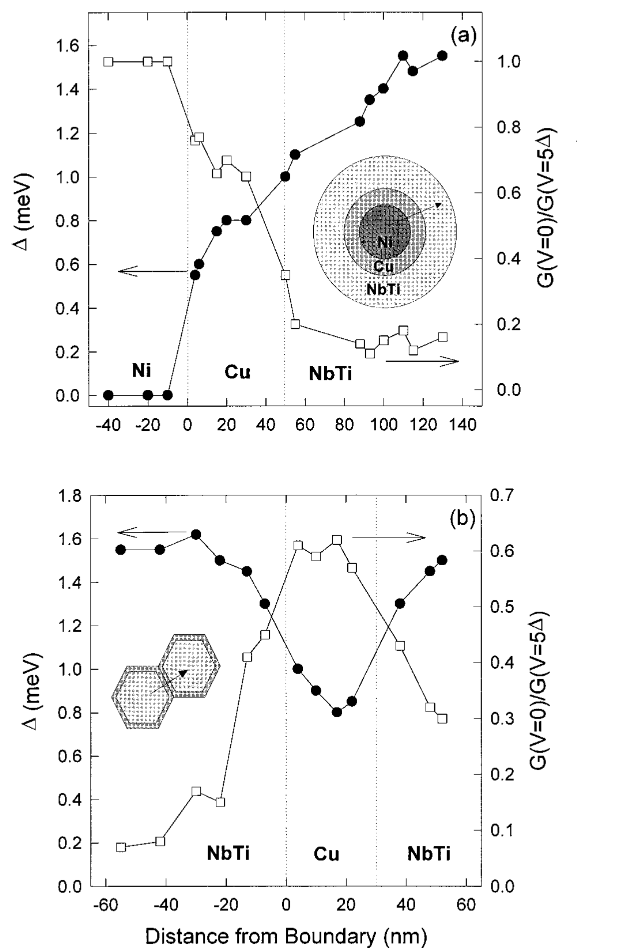

FIG. 3. (a) Spectroscopic gap, Δ (black circles, left axis) and normalized ZBC (white squares, right axis) data taken on the Ni island pin wire as a function of distance from the Ni/Cu interface. Boundaries between different types of materials are designated by vertical dashed lines. The experimental errors on the data are approximately the size of the symbols. (Inset) Diagram of the area studied, with an arrow illustrating the scan line on which the $I-V$ curves were taken. (b) Same as (a), but for the Cu barrier-pin wire. Note the difference in scales and that the scan line crosses two Cu/NbTi boundaries.

has the ''island-type'' pin geometry and uses a ferromagnetic pin. The ''unit filament'' consists of a pin placed inside a NbTi cylinder. After numerous steps of extrusion and drawing, the NbTi cylinder is reduced to 1 μm in diameter. Each pin consists of a cylindrical Ni filament 200 nm in diameter, surrounded by a 50 nm thick Cu sleeve which serves as a diffusion barrier against the migration of Ni into NbTi. A sample micrograph of a single Ni island pin wire is shown in Fig. 1. The second wire [Figs. 2 and 3(b)] has the ''barrier-pin'' geometry where the unit filament is a NbTi hexagon 80 nm in size, surrounded by a 15 nm thick Cu barrier. The pin is Cu, a normal metal. Both wires consist of an ordered array of such unit filaments inside a Cu cladding. The motivation for the choice of these two wires is twofold: first, the wires differ considerably in their fine-structure dimensions and second, one of the wires includes a ferromagnetic constituent, which is inimical to superconductivity.

After polishing and etching the surface, STM topographic images of the wire cross section were taken at 4.2 K simultaneously with current–voltage ($I-V$) characteristics at different lateral tip positions. By employing this method we could study the local DOS (via the dI/dV vs V curves) in correlation with the surface structure. In particular, we mapped the DOS as a function of the distance from the interface between different materials. In Fig. 2(a) we plot four experimental tunneling $I-V$ curves (fuzzy lines) taken at different positions along the Cu barrier-pin wire, as indicated in the topographic image [Fig. 2(b)]. The image is presented in gray scale, where dark corresponds to depressed areas and bright to elevated ones. It focuses on a small section of a Cu barrier-pin [depressed due to differential etch rates] sandwiched between two NbTi regions, on the upper left and lower right parts of the image. The change in the local DOS is manifested in Fig. 2(a). One can see (curve 1) that deep in the S side a large spectroscopic gap is apparent, but when approaching the Cu (darker area) from inside the NbTi the gap diminishes (curve 2). In the Cu region a gap is clearly observed, although smaller than in the NbTi (curve 3). Finally, the gap recovers after entering the adjacent NbTi filament (curve 4). We point out that we measured both wires also at ~ 10 K (just above $T_C \approx 9$ K), and then *only* gapless $I-V$ curves were found all over the samples, indicating that the gaps present at 4.2 K, *both in NbTi and Cu*, are of superconducting origin, and not due to extraneous effects.

The parameters which can be extracted from the data are the magnitude of the gap and the zero bias conductance (ZBC) normalized to the conductance at a high bias. We interpret the occurrence of a large gap, combined with low ZBC, as a signature of the local effect of superconductivity while a small or vanishing gap and a normalized ZBC close to unity signify normal metallic behavior.

As an initial approach to data analysis, to obtain an estimate of the gap we fit the experimental $I-V$ and dI/dV vs V curves using the conventional[4] tunneling expressions for N-S tunnel junctions, taking the DOS introduced by Dynes *et al.*[11] Δ designates the superconducting gap and Γ is a phenomenological quasi-particle lifetime broadening, typically 30% of Δ. Although this approach does not give a complete description of the data, it provides a consistent way to quantitatively assess the magnitude of the gap. The theoretical fits are satisfactory as long as one seeks the *general* behavior of the gap, as can be seen in Fig. 2(a). However, they cannot account for subtler features which are *usually* present, in particular an enhancement of the DOS at the gap edge and minor peaks in the derivative (dI/dV) above Δ. These may be attributed to quasi-particle bound states, multiple Andreev reflections at the material boundaries, and to phonon structure. These features are observed in the dI/dV traces plotted in the inset of Fig. 2(a). The theoretical fits indeed deviate from the experimental data around the peaks (due to DOS enhancement), and do not account for the detailed structure above the gap [see lower curve and the corresponding fit (dotted line)]. These latter issues require a more thorough theoretical treatment[7,8] which will be pursued subsequently. Nevertheless, the general picture is clear.

Figures 3(a) and 3(b) show the variations of the gap, Δ, and the ZBC as a function of the distance from the boundaries for the two wires. The insets illustrate the direction along which the $I-V$ curves were taken, and the various materials along each line. One can see from Fig. 3(a) that inside the Ni the $I-V$ curves are ohmic ($\Delta = 0$; ZBC$=1$) but in the Cu sleeve, *adjacent to the Ni*, we already find indications of a gap. As the NbTi is approached from inside the Cu, the gap increases and the ZBC diminishes. This trend continues inside the NbTi with growing distance from the pin, until saturation values of $\Delta = 1.55$ meV (yielding the established[4] ratio for NbTi, $2\Delta/k_BT \sim 4$) and ZBC$=0.15$ are reached at about 50–60 nm from the NbTi–Cu interface. The healing length in the Cu barrier-pin wire, namely the distance from the Cu–NbTi interface over which Δ attains its bulk value, is found to be shorter—about 30–40 nm—as demonstrated in Fig. 3(b). Here too, superconductivity is monotonically suppressed in the NbTi as the Cu–NbTi interface is approached. Δ continues to decrease within the Cu region, reaching its minimal value approximately midway between the two adjacent S filaments, as expected.

The origin of the gap and the value of Δ we extract do not lend themselves to an easy interpretation, in particular not in N. Close to the interface the gap in N should be affected by intermixing. However, far enough from the boundary, where intermixing effects are negligible, the gap in N is probably due mainly to leakage of Cooper pairs and quasi-particles from S to N. This is consistent with the dirty limit approximation for the PE,[4] yielding a Cooper pair (order parameter) penetration length of $\sim 50-100$ nm into the Cu. It is also consistent with the fact that the gap is completely suppressed in the ferromagnetic Ni region, due to pair breaking.[12] A single quasi-particle bound state of energy close to the superconducting gap of NbTi may also lead to a similar gap structure.[8] However, this is not likely to be the case here, since the boundaries are not specular at the nanometer scale and the magnitude of the measured gap varies spatially along the Cu. The gap in S, on the other hand, is directly related to the local pair potential.

We find that superconductivity is suppressed in NbTi near the interface with Cu, and its healing length in the (ferromagnetic) Ni island-pin wire (50–60 nm) is larger than in the Cu barrier wire (30–40 nm). An important result is that these lengths are *much larger* than the superconducting coherence length in NbTi at 4.2 K, $\xi_S \sim 5$ nm.[13] This can be attributed to intermixing of materials at the interfaces, which could have occurred during fabrication. However these large healing lengths, along with the substantial difference between the two wires, may be partly due also to a strong PE induced by Cu which can be further enhanced by the presence of the Ni filament. Our data *cannot* be explained by bad electrical contact between S and N, as we recall[10] that in the case of bad electrical contact and no intermixing, the healing length of superconductivity inside S is comparable to ξ_S, and gaps hardly appear in the N regions. Further studies, in particular—measurements in magnetic fields, are needed in order to clarify this problem and assess the origin of the gap in the normal regions.

The authors thank J. Q. Wang for helpful discussions. This work was supported by the CT-Dept. of Economic Development and IGC-AS.

1. L. R. Motowidlo, B. A. Zeitlin, M. S. Walker, and P. Haldar, Appl. Phys. Lett. **61**, 991 (1992); N. D. Rizzo, J. Q. Wang, D. E. Prober, L. R. Motowidlo, and B. A. Zeitlin, *ibid.* **69**, 2285 (1996).
2. R. W. Heussner, J. D. Marquandt, P. J. Lee, and D. C. Larbalestier, Appl. Phys. Lett. **70**, 901 (1997).
3. G. Deutscher and P. G. de Gennes, in *Superconductivity*, edited by R. D. Parks (Dekker, New York, 1969), Vol. 2.
4. E. L. Wolf, *Principles of Electron Tunneling Spectroscopy* (Oxford University Press Oxford, 1989).
5. A. C. Mota, P. Visani, A. Pollini, and K. Aupke, Physica B **197**, 95 (1994).
6. V. Petrashov, V. N. Antonov, P. Desling, and T. Cleason, Phys. Rev. Lett. **74**, 5268 (1995); H. Courtois, Ph. Gandit, D. Mailly, and B. Pannetier, *ibid.* **76**, 130 (1996).
7. S. Gueron, H. Pothier, N. O. Birge, D. Esteve, and M. H. Devoret, Phys. Rev. Lett. **77**, 3025 (1996).
8. S. H. Tessmer, D. J. Van Harlingen, and J. W. Lyding, Phys. Rev. Lett. **70**, 3135 (1993); S. H. Tessmer, M. B. Tarlie, D. J. Van Harlingen, D. L. Maslov, and P. M. Goldbart, *ibid.* **77**, 924 (1996).
9. K. Inoue and H. Takayanagi, Phys. Rev. B **43**, 6214 (1991).
10. O. Millo, Y. Levi, E. Bar-Sadeh, U. Asaf, and I. Felner, J. Low Temp. Phys. **106**, 417 (1997).
11. R. C. Dynes, V. Naraynamurti, and J. P. Garno, Phys. Rev. Lett. **41**, 1509 (1978).
12. J. Q. Wang, N. D. Rizzo, D. E. Prober, L. R. Motowidlo, and B. A. Zeitlin, IEEE Trans. Appl. Supercond. **7**, 1130 (1997).
13. X. S. Ling, J. D. McCambridge, N. D. Rizzo, J. W. Sleight, D. E. Prober, L. R. Motowidlo, and B. A. Zeitlin, Phys. Rev. Lett. **74**, 805 (1995).